SuperDARN and IMAGE WIC observations during intervals of steady magnetospheric convection

K.A. McWilliams, J.B. Pfeifer, R.L. McPherron, and H.U. Frey

Abstract: If steady magnetospheric convection (SMC) occurs when the magnetosphere is in a relatively steady state of flux transfer, i.e., dayside and nightside reconnection is balanced, then signatures of magnetic reconnection that are commen to the dayside magnetosphere may be observable on the nightside also. Magnetic reconnection on the dayside produces relatively clear data signatures, such as reconnection-associated field-aligned currents (FACs), the reconnection electric field and associated convection, and energy-dispersion of precipitating ions. The processes involved produce these clear signatures, because the dayside magnetosphere is less distorted and there exists more direct connection to the solar wind driver than the nightside magnetosphere. The more global scale convection and current patterns, such as the Region 1 and 2 FACs, develop when the dayside magnetosphere is controlled by a moderately steady solar wind driver for a longer period. We present examples of energy-dispersed ions in the substorm sector during an interval of SMC, and we also discuss inferred FAC patterns based on the combined auroral images and convection patterns.

Key words: steady magnetospheric convection, magnetosphere, field-aligned currents.

1. Introduction

In any physical system the characteristics of the stability of that system is of fundamental importance to understanding the system's behaviour. The Earth's magnetosphere is an open system that is driven by its interaction with the solar wind. The dynamics of the magnetosphere is therefore a function of the upstream driver. The solar wind is not a steady, continuous stream of plasma from the Sun, so the magnetosphere finds itself in a highly variable space plasma environment. The variability of the upstream driver results in variability of convection in the magnetosphere, which is further complicated by internal processes intrinsic to the magnetosphere itself that also affect its dynamics. The result is a complex interaction between internal and external processes.

Steady magnetospheric convection (SMC) [10] events are intervals of enhanced convection without any classical substorm signatures (see [12] and references therein). When the magnetosphere is driven to this relatively steady state, there is, effectively, a balance between the creation of open flux on the dayside and the closure of flux on the nightside. Magnetospheric convection maps down to ionospheric altitudes, where the plasma drift can be measured by SuperDARN [3]. Global ionospheric convection maps are created by assimilating data from all available SuperDARN radars, and these can be used to quantify convection in the magnetosphere. Currents in the magnetosphere and ionosphere induce ground magnetic perturbations, which are detected by networks of ground magnetometers. Magnetic activity indices, such as the auroral electrojet (AE) index, quantify the activity of the magnetosphere, and they are also one of the substorm indicators.

Received 25 May 2005.

K.A. McWilliams and J.B. Pfeifer. Dept. of Physics & Engineering Physics, University of Saskatchewan, Saskatoon, Canada
R.L. McPherron. Institute for Geophysics and Planetary Physics, University of California, Los Angeles, CA, USA
H.U. Frey. Space Sciences Laboratory, University of California, Berkeley, CA, USA

2. SMC selection: Statistics

One of the more commonly used set of criteria for systematically selecting SMC intervals was presented by [11], and this scheme included: requirements of the orientation of the upstream IMF, enhanced convection determined using the AE and AL indices, and no ground or in situ magnetotail substorm signatures.

The criteria of [11] require extensive data collection and analysis, which was not easily automated, so we have chosen to use the use the more recent and entirely ground-based definition of SMC of [1], which is based solely on the behaviour of the AE and AL indices. In the present study, SMC was deemed to have occurred when the AE and AL indices satisfied the following criteria for a minimum of three hours: (a) AE index values larger than 200 nT to ensure active conditions, and (b) the AL index did not decrease at a rate faster than 25 nT per minute to ensure no substorm onset. These criteria effectively select the longer intervals of [1].

The number of events, as a function of months, for years between 1990 and 2001 are presented in Fig. 1. The total number of SMC intervals in a year ranged from about 10 to 50. The number of SMC events appears to depend on both the solar cycle and the season. More events were detected near solar maximum, as would be expected because of the more active solar and geomagnetic conditions at these times. More events were detected during the northern summer months. This appears to be the result of the way that the AE and AL indices are derived, as discussed by [6], rather than a geophysical process. The AE and AL indices are determined using solely northern hemisphere auroral region magnetometers, which respond to changes in the northern auroral electrojet currents. The magnitude of these currents depends strongly on the conductivity of the ionosphere, which is affected in a large part by the amount of sunlight impinging on the upper atmosphere. During the northern summer months the conductivity in the northern ionosphere is higher than during the northern winter months. The higher conductivity produces larger currents and therefore larger AE values during the summer months. If there

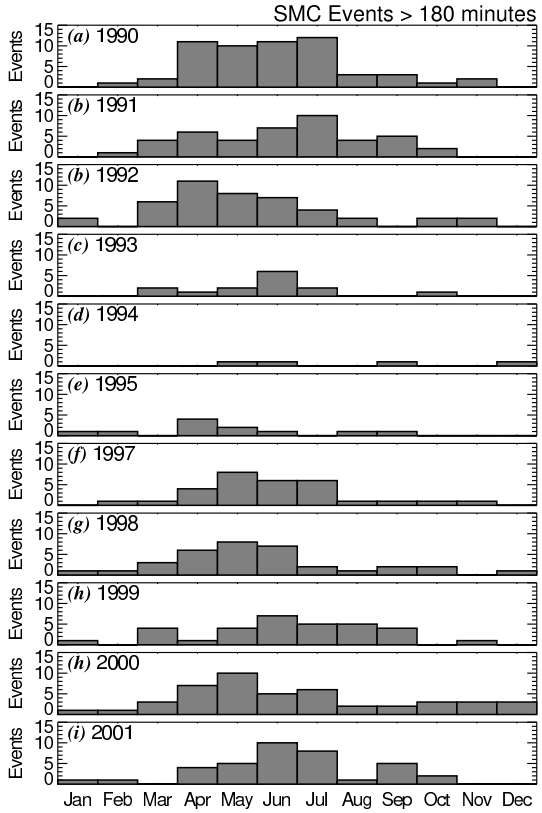

Fig. 1. The number of SMC intervals selected for each month during selected years between 1990 and 2001, inclusive.

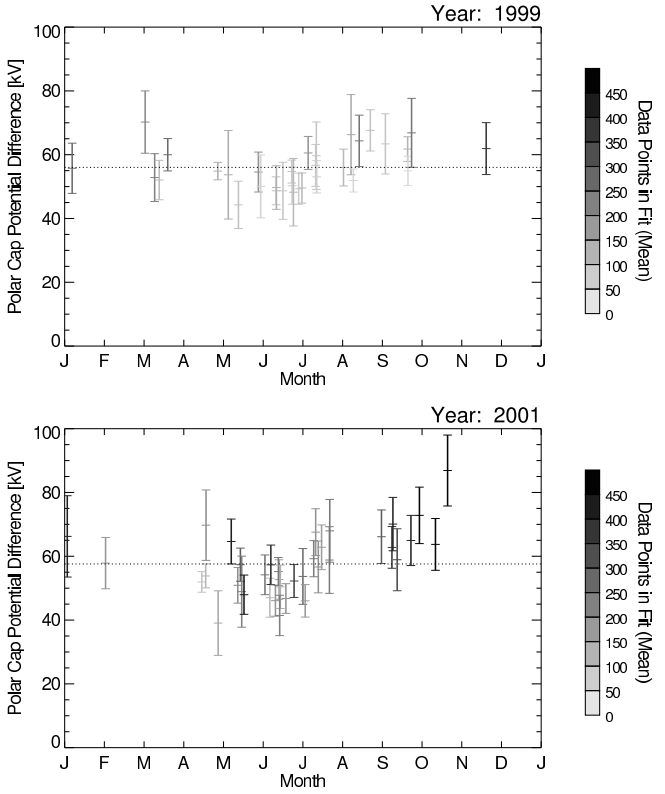

Fig. 2. The mean polar cap potential difference Φ_{PC}, plus or minus one standard deviation, for all SMC intervals in 1999 and 2001. The greyscale indicates the mean number of SuperDARN velocity data points used to produce each map during each SMC interval.

were an analogous AE index in the southern hemisphere we would expect to observe the opposite bias, with more events in the winter months.

For the solar maximum years presented in Fig. 1, lowering the minimum AE threshold from 200 nT to 80 nT resulted in roughly 10-12 events detected during the winter months. Varying the AE threshold between 80 and 200 nT during the year could reduce the northern summer bias.

3. SuperDARN global convection during SMC

SuperDARN global convection maps were produced for the 1999 and 2001 SMC events. (Note that for 2001 there are no AE/AL data in November and December, so the apparent lack of events is not a geophysical effect.) The northern hemisphere convection maps were produced every two minutes, using all available data. The polar cap potential difference Φ_{PC} is directly related to the strength of the ionospheric convection, so we have used Φ_{PC} averaged over the SMC interval to quantify the magnetospheric convection for that interval. The mean Φ_{PC} values for each SMC event are presented in Fig. 2, plus or minus one standard deviation. The greyscale indicates the number of data points in the SuperDARN convection maps, and this value is obtained by averaging the number of points in a two-minute map over the entire SMC interval. The yearly mean of Φ_{PC} is nearly 60 kV for both 1999 and 2001, but the mean voltage appears to be lower in the summer than in the winter. This is consistent with the seasonal dependence of SMC occurrence rate. During the northern winter months, when the conductivity is reduced, stronger convection (and therefore higher transpolar voltage) is required to produce larger currents to achieve the AE$>$200 nT threshold.

It is interesting to note that during all SMC intervals when global SuperDARN convection patterns were calculated, the number of SuperDARN data points was relatively large. Some maps included more than one thousand data points. This increases confidence in the fitting techniques used to determine the equipotential contours. We have yet to determine if this excellent data coverage is characteristic of SMC intervals, and we intend to investigate this in more detail.

4. Case study: 2001/01/03, 02:57-06:46 UT

This case study, which occurred between 02:57 and 06:46 UT on 3 January 2001, was the first of the SMC events found in 2001. At the SMC onset the AL index drops weakly in a manner that is similar to a weak substorm, but the AL value decreases at a rate less than 25 nT per minute, and so it satisfies the SMC selection criteria. In contrast to a more typical substorm, the AE index remains high for nearly 4 hours. This SMC interval has the appearance of a weak substorm with a prolonged recovery phase. SuperDARN convection patterns were available for the duration of the event, and IMAGE WIC images [8] were available from prior to the onset until about

05:30 UT.

4.1. IMF conditions

The IMF data for this case study are presented in Fig. 3. A simple ballistic time delay from ACE was calculated to be 73 minutes, using a speed of 350 km s^{-1} and a distance of 240 R_E. The lagged SMC interval is plotted as vertical dashed lines. The IMF was relatively steady and moderate during this SMC interval, but the high solar wind concentration of nearly 40 cm^{-3} shortly before onset and $\sim$20 cm^{-3} during the first half of the SMC interval suggests this SMC occurred during a magnetic cloud event. The values of the other solar wind parameters were less unusual. The IMF B_z component rotates from -10 nT to +5 nT, as expected for a magnetic cloud.

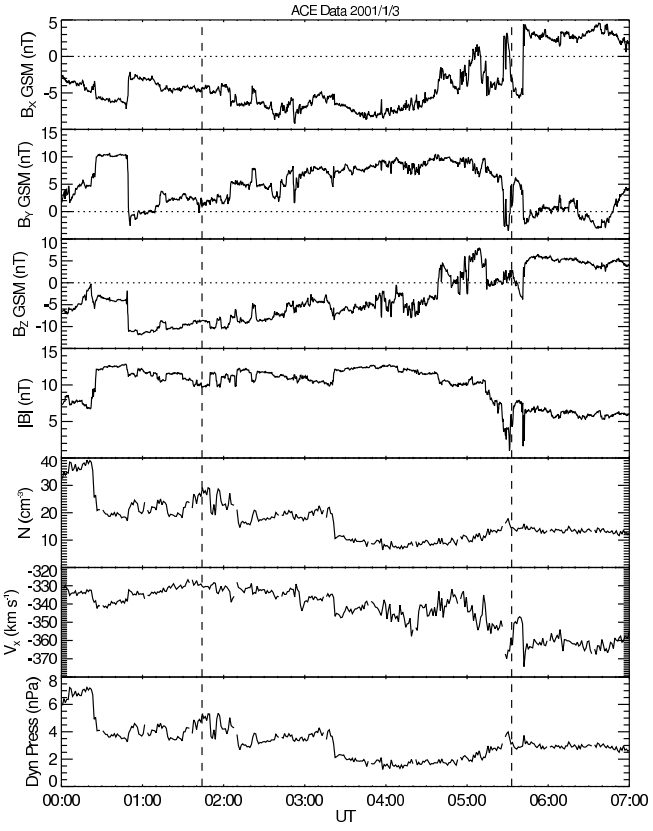

Fig. 3. The IMF and solar wind data measured from 00-07 UT on 03 January 2001.

4.2. Dayside convection driver

Energy dispersed cusp ions (not shown) were observed by several of the DMSP satellites thoughout the duration of this SMC interval. This provides strong evidence of continual open flux loading on the dayside throughout the entire interval. Cusp ions were measured over a very large range of magnetic local times on the dayside, $\sim$7 hours of MLT, indicating that merging on the dayside was occurring over vast portions of the frontside magnetopause prior to and during the SMC event. The very extensive dayside reconnection footprint provides evidence of substantial opening of flux on the dayside, which continually replenishes the open flux in the polar cap that is lost to reconnection on the nightside, thereby maintaining a relatively steady amount of open flux in the polar cap.

4.3. Nightside convection and aurora

Several examples of combined convection and aurora plots from this event are presented in Fig. 4. These data were measured (a) near the onset of SMC, (b) approximately one hour after the SMC onset, and (c) 3.5 hours after SMC onset, when the double oval had fully developed. These particular images were selected because they coincided with DMSP passes near local midnight. The corresponding DMSP particle spectrograms are presented in Fig. 5.

The flow out of the polar cap shortly after the SMC onset occurred between 21 and 23 MLT in the region of bright aurora, as show in Fig. 4(a). The flow had a zonal component towards earlier local times. The DMSP F15 spacecraft traversed the midnight auroral zone in the southern hemisphere, and the conjugate footprint in the northern hemisphere crossed the eastern end of the bright aurora near midnight. DMSP F15 encountered auroral precipitation between 03:18 and 03:22 UT. Energy dispersed ions were first encountered near the poleward edge of the bright aurora (see Fig. 5(a)). The low-energy cutoff exhibits an energy dispersion with lower cutoff energies observed at lower latitudes. This energy dispersion was observed over several degrees of magnetic latitude, over distances at least as large as the latitudinal width of the auroral oval.

Nearly an hour after the start of the SMC interval (Fig. 4(b)), the double oval is not yet fully developed, but there exists a marked difference in luminosity between the poleward and equatorward regions of the auroral oval, with the poleward portion being significantly brighter. The bright poleward aurora occurred near the premidnight convection reversal boundary, as expected for a region of downward FAC and therefore diverging electric field. DMSP F12, whose magnetically conjugate trajectory is presented in Fig. 4(b), began to measure ion flux near the poleward edge of the bright northern aurora (Fig. 5(b)), but the more obvious energy dispersion did not begin until roughly 03:52 UT. The minimum ion cutoff energy decreased with decreasing magnetic latitude, as before.

The double oval, a common feature of SMC and of the substorm recovery phase (e.g., see [4]), is now fully developed, as evident in Fig. 4(c). The auroral images at this time suffer from significant distortion in the postmidnight sector, because of the oblique viewing angle of IMAGE WIC. DMSP F12 performed a skimming orbit of the auroral region (in the southern hemisphere), so it is difficult to determine with great precision where the ion energy dispersion began in Fig. 5(c). There was a strong flux of ions that coincided with the equatorward oval, and the energy dispersion becomes evident from near the poleward edge of the equatorward oval. The region of convection out of the polar cap has shifted slightly toward midnight. It is important to note that the IMF orientation has begun to change around this time.

5. Discussion

Smaller scale (of the order of $\sim$100 km or less) energy dispersion features in the precipitating particles in the substorm sector have been examined (e.g., [5]), but we are considering

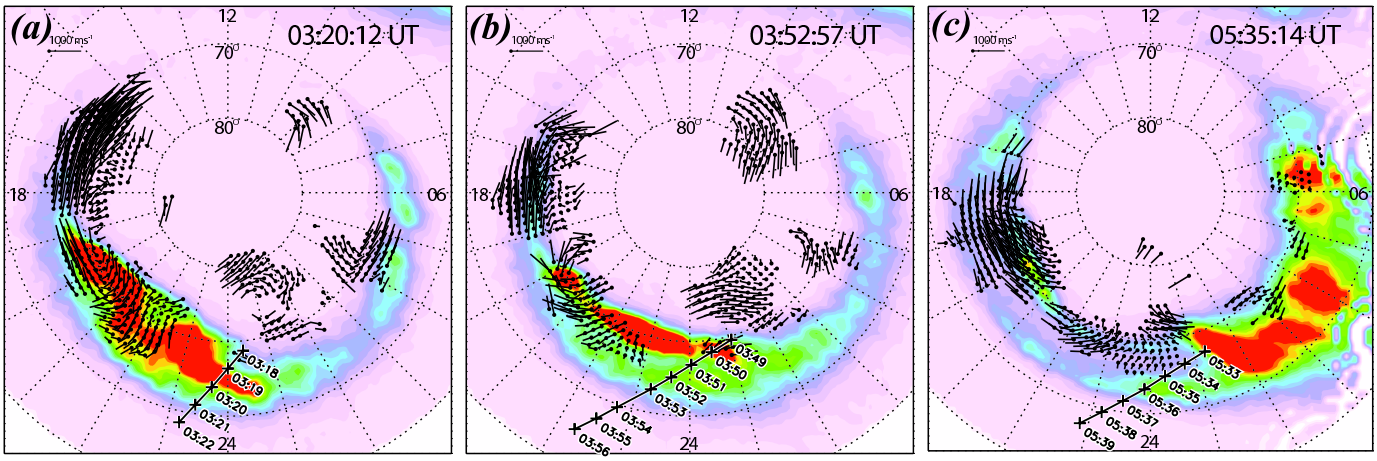

Fig. 4. The (a) 03:20:12 UT, (b) 03:52:57, and (c) 05:35:14 UT IMAGE WIC auroral image, overlaid with the corresponding two-minute SuperDARN convection velocities. DMSP trajectories in the substorm sector are indicated with the black line, with crosses denoting specific times along the trajectory, as listed.

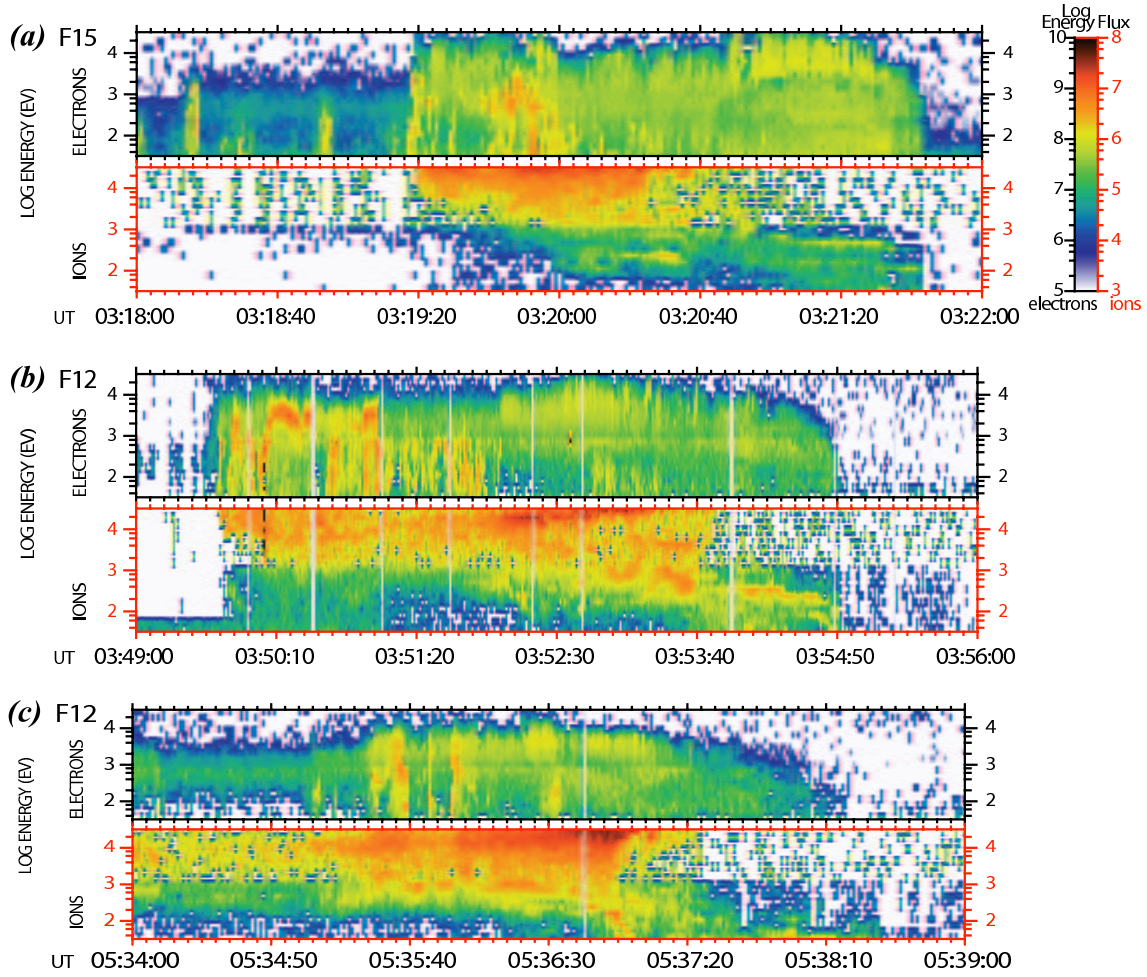

Fig. 5. The DMSP electron and ion particle spectrograms from the nightside passes, which correspond to the panels in Fig. 4. The location of the spacecraft are indicated in Fig. 4.

here the global magnetosphere response during SMC and we are concentrating on energy-dispersed ions that extended over several degrees of magnetic latitude. These large-scale ion energy features have been presented in previous studies, but they have not been noted. For example [9] presented FAST particle observations during substorm aurora, and the particles exhibited a clear energy dispersion with a low-energy cutoff. The highest cutoff energies were observed near the poleward edge of the auroral oval, and the cutoff energy decreased as the spacecraft moved equatorward. These observations are very consistent with our SMC nightside ions, and we propose a simple nightside velocity filter effect picture, analogous and consistent with dayside models, that could explain the large-scale signatures that we observed during SMC.

Models of dayside convection and FACs, and their dependence on IMF B_y, were presented by [2]. We have adapted their dayside convection and FAC diagram to the nightside, assuming that the magnetosphere could reach some equilibrium convection state, which is what we believe SMC approaches. The top panel in Fig. 6 most closely approximates our observations in the 03 January 2001 case study. In general, the SuperDARN convection pattern revealed flows out of the polar cap that were tilted towards earlier local times during most of the SMC interval. The fitted convection patterns did not exhibit such a pronounced Harang Discontinuity as this simplified model, and this may or may not be due to data coverage and quality in the fitted equipotential contours in the dawn convection cell. The configuration of the tail magnetic field is also highly complex, which will lead to deviations from this simple picture of the footprint of magnetospheric convection.

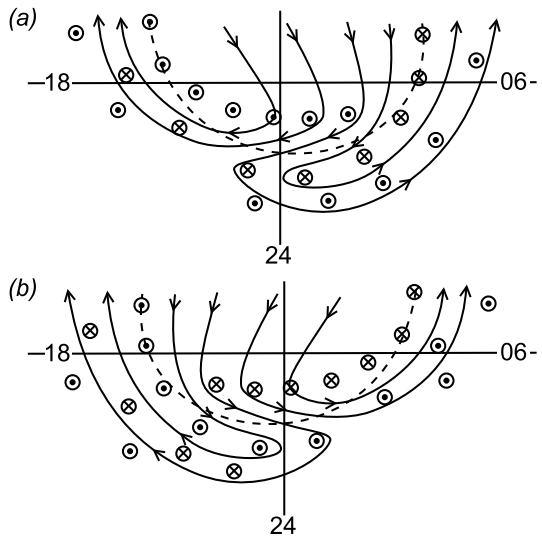

Fig. 6. A proposed pattern of nightside convection and FACs during SMC. The dashed line indicates the approximate expected location of the polar cap boundary.

The direction of the FACs in Fig. 6 are predicted primarily based on the proposed convection pattern. The vorticity of the plasma convection is an indicator of the general direction of FAC flow [13]. In the northern hemisphere, downward vorticity (including both vortical and shear flow) corresponds to upward FAC, and vice versa. The recorded development of the double oval is consistent the top panel in Fig. 6. It is important to note that the very clear double oval, with two large and distinct bands of aurora, was observed at local times earlier than $\sim$02 MLT. When compared with Fig. 6(a), one can see that there are two upward FAC bands that flank a downward FAC band. This is only a very simple comparison for an idealized situation. In reality, the bright aurora also indicates regions of enhanced conductivity and conductivity gradients, which modify and refine the estimated FAC distributions.

The dashed line in Fig. 6 represents the open-closed field line boundary, and this is also consistent with DMSP particle spectrograms. The most energetic energy-dispersed ions appeared in the vicinity of the poleward FAC band, near the polar cap boundary, and the ions exhibited decreasing energy with decreasing latitude, as expected. One would expect that the most recently reconnected flux tubes would have precipitating ions with the highest minimum energy, with ever decreasing minimum energies observed as the flux tubes convect out of the polar cap.

5.1. Preferred Dayside Merging Site

Why might one expect convection to be directed towards the premidnight sector? One must consider the accumulation of open flux in the magnetotail, as controlled by the IMF orientation. In the event presented, when there were both auroral images and convection maps, the magnitudes of the three IMF components were comparable (see Fig. 3), with $B_z < 0$, $B_y > 0$, and $B_x < 0$.

Preferred magnetopause merging sites for positive IMF B_y are expected at high latitudes – a prenoon southern hemisphere region and a postnoon northern hemisphere region. The presence of a strongly negative IMF B_x would tend to favour the southern prenoon site, which is the case shown in Fig. 7. Fig. 7 is an idealized artistic rendering of the frontside magnetopause, adapted from [14]. An IMF line ("1") with negative B_z and

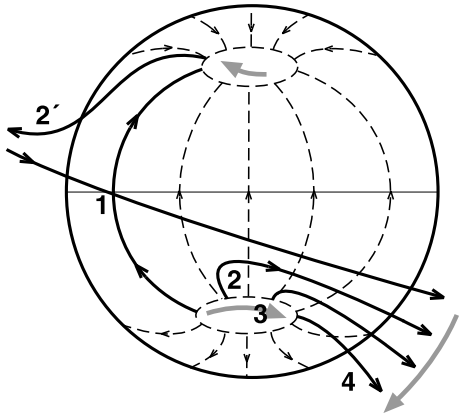

Fig. 7. Evolution of magnetic field lines following reconnection at a southern prenoon high-latitude site. Figure modified from the original version of [14] The numbers indicate the temporal evolution of the flux tube following reconnection, with the primed numbers mapping to the northern hemisphere and the unprimed numbers mapping to the southern hemisphere.

positive B_y approaches the geomagnetic field. Following reconnection the flux tubes convect away from the reconnection

site, and the subsequent positions of the flux tube are denoted by the numbers, with the "primed" flux tubes mapping into the northern ionosphere and the "unprimed" flux tubes mapping to the southern.

This gives rise to southern hemisphere prenoon flux tubes convecting towards the postnoon magnetotail in the southern hemisphere and the prenoon magnetotail in the northern hemisphere, under the influence of the positive IMF B_y component. This asymmetric accumulation of open flux in magnetotail would be expected to give rise to asymmetric convection patterns in the ionosphere. The accumulation of more flux in the northern postmidnight tail would lead to the convection in the northern hemisphere towards earlier local times following reconnection. We would expect the opposite to be true for the southern hemisphere, and preliminary analysis of the southern hemisphere SuperDARN data (not shown) support this hypothesis, with convection out of the southern polar cap directed towards later local times.

6. Summary and conclusions

The particle, aurora and convection observations were all consistent with the model of ionospheric convection and FACs presented in Fig. 6(a). Because SMC intervals are believed to approach as steady a state as one might expect of magnetospheric convection, we believe that SMC intervals are ideal to deduce properties of the magnetospheric state towards which the magnetosphere tends regardless of whether it is driven in a steady or irregular manner.

We identified SMC intervals with a minimum duration of three hours using the criteria of [1]. The occurrence statistics displayed a seasonal and solar cycle dependence, such that more active and more sunlight times had more SMC intervals. The strength of the ionospheric convection, quantified using Φ_{PC}, also displayed a seasonal dependence consistent with the SMC occurrence rates, such that stronger convection was required during the dark northern winter to achieve the same auroral electrojet currents as in the sunlit northern summer months.

SuperDARN had very good data coverage in the premidnight and midnight sector during our case study of 03 January 2001. The flow out of the polar cap was observed in the premidnight sector for the majority of the interval, and the flow was directed towards earlier local times coming out of the polar cap. This is believed to be consistent with the asymmetric accumulation of open flux in the tail lobes as a result of dayside occurring at a prenoon, high-latitude southern hemisphere merging site.

The IMAGE WIC images showed the development of a double auroral oval during the SMC case study. This is consistent with two bands of upward FAC poleward and equatorward of a band of downward FAC. The vorticity of the SuperDARN convection patterns, which is an estimator of FAC direction, was consistent with the regions of bright aurora.

Several DMSP passes through the midnight sector showed clear energy dispersion of precipitating ions, consistent with the velocity filter effect on recently reconnected field lines.

References

1. O'Brien, T.P., Thompson, S.M., and McPherron, R.L., Steady magnetospheric convection: Statistical signatures in the solar wind and AE, *Geophys. Res. Lett., 29:7*, 10.1029/2001GL014641, 2002.
2. Cowley, S.W.H., and Lockwood, M., Excitation and decay of solar wind-driven flows in the magnetosphere-ionosphere system, *Ann. Geophys., 10*, 103–115, 1992.
3. Greenwald, R.A., et al., DARN/SuperDARN: A global view of high-latitude convection, *Space Sci. Rev., 71*, 763–796, 1995.
4. Henderson, M.G., Reeves, G.D., Skoug, R., Thomsen, M.F., Denton, M.H., Mende, S.B., Immel, T.J., Brandt, P.C., and Singer, H.J., Magnetospheric and auroral activity during the 18 April 2002 sawtooth event, *J. Geophys. Res., 111:A01S90*, doi:10.1029/2005JA011111, 2006.
5. Lockwood, M., Identifying the open-closed field line boundary, *in Polar Cap Boundary Phenomena,* edited by J. Moen et al., pp. 73–90, Kluwer Academic Publishers, Netherlands, 1998.
6. McPherron, R.L., O'Brien, T.P., and Thompson, S.M., Solar wind drivers for steady magnetospheric convection, *in Multiscale Coupling of Sun-Earth Processes*, edited by A.T.Y. Lui, Y. Kamide, and G. Consolini, pp. 113–124, Elsevier, Amsterdam, 2005.
7. Ruohoniemi, J.M., Baker, K.B., Large-scale imaging of high latitude convection with Super Dual Auroral Radar Network HF radar observations, *J. Geophys. Res., 103*, 20797–20811, 1998.
8. Mende, S.B., et al., Far ultraviolet imaging from the IMAGE spacecraft. 3. Spectral imaging of Lyman-α and OI 135.6nm, *Space Sci. Rev., 91:1-2*, 287–318, doi:10.1023/A:1005292301251, 2000.
9. Mende, S.B., Frey, H.U., Carlson, C.W., and McFadden, J., IMAGE and FAST observations of substorm recovery phase, *Geophys. Res. Lett., 29:12*, 10.1029/2001GL013027, 2002.
10. Pytte, T., McPherron, R.L., Hones, J.E.W., and West, J.H.I., Multiple-satellite studies of magnetospheric substorms, III. Distinction between polar substorms and convection-driven negative bays, *J. Geophys. Res., 83:A2*, 663–679, 1978.
11. Sergeev, V.A., and Lennartsson, W., Plasma sheet at X $\sim$ -20 R_E during steady magnetospheric convection, *Planet. Sp. Sci., 36:4*, 353-370, 1988.
12. Sergeev, V.A., Pellinen, R.J., and Pulkkinen, T.I., Steady magnetospheric convection: A review of recent results, *Space Sci. Rev. 75*, 551–604, 1996.
13. Sofko, G.J., Greenwald, R.A., and Bristow, W.A., Direct determination of large-scale magnetospheric field-aligned currents with SuperDARN, *Geophys. Res. Lett., 22*, 2041–2044, 1995.
14. Wild, J.A., et al., Coordinated interhemispheric SuperDARN radar observations of the ionospheric response to flux transfer events observed by the Cluster spacecraft at the high-latitude magnetopause, *Ann. Geophys., 21*, 1807–1826, 2003.